Altai State University

Cosmic Ray Mass Composition Problem:

towards model-independent evaluation based on the analysis of the spatial and temporal structure of EAS charged components

R. I. Raikin, A. A.Lagutin, T. L. Serebryakova, N. V. Volkov, S. V. Soldatkin , E. M. Palkowski

3rd International Symposium on Cosmic Rays and Astrophysics (ISCRA-2021). MEPhI, June 08–10, 2021

Plan

1. **Current state of the mass composition problem**
   - Main constraints and possible way-outs
2. **Scaling formalism for lateral distributions**
   - Limitations and generalizations
   - Implementations at moderate energies
   - Perspectives for extremely-high energies
3. **Universality**
   - Implementation for different EAS arrays
4. **Conclusions**

Cosmic ray spectrum

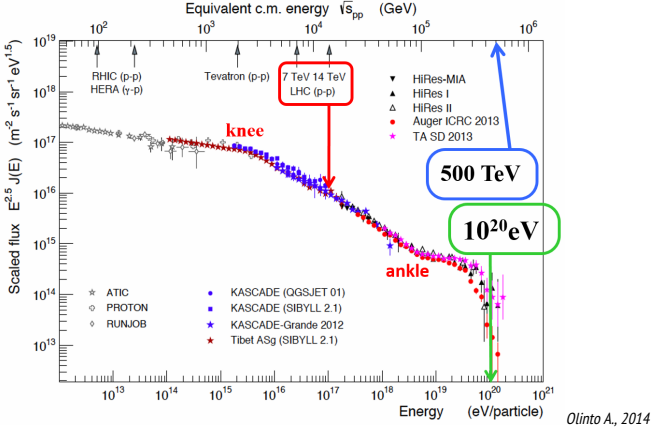

Olinto A., 2014

GALACTIC ??? EXTRAGALACTIC?

Flux < 1 particle/km^2/century at $E > 10^{20}$ eV

Detection via Extensive Air Showers registration

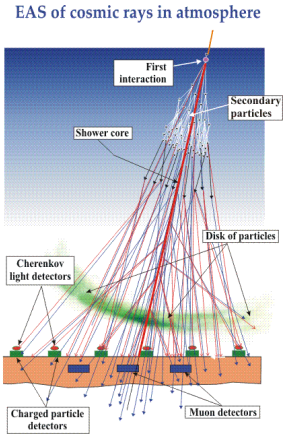

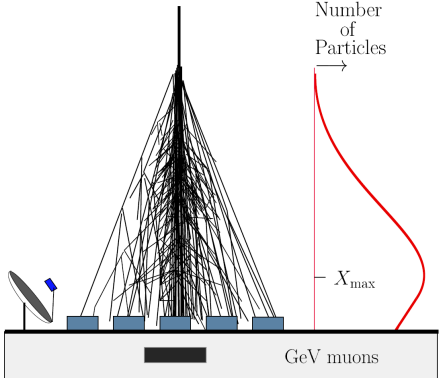

Anchordoqui L. et al., 2003

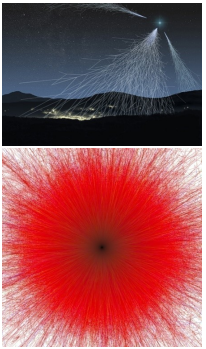

Bret L./Novapix/ASPERA

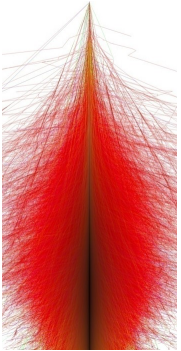

www-ik.fzk.de/corsika

Shower parameters are reconstructed by comparing observational data with results of detailed simulations

Reliable precise mass composition evaluation is crucial for the interpretation of the experimental data in terms of sources and propagation models

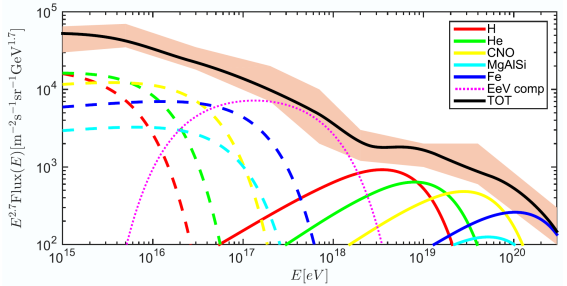

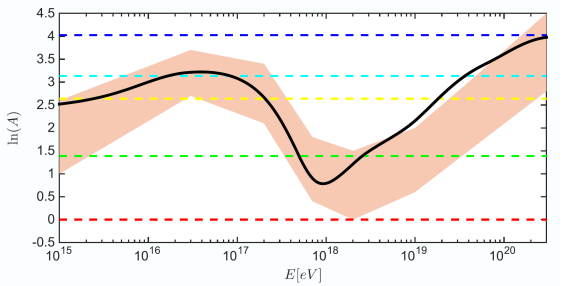

Model particle fluxes for different spieces and predicted average atomic mass as a function of energy (*Caprioli D., 2015*)

Basic methods and techniques for primary mass estimations

Analysis of mean values, fluctuations, correlations or even particular features of distributions of different air shower observables characterized both longitudinal and spatial shower development

- ✓ Depth of maximum of the cascade curve $X_{\max}$
- ✓ Total number of electrons N_e and muons N_μ at the observation level, their correlation, muon size in inclined showers
- ✓ Local densities of electrons $\rho_e(r)$ and muons $\rho_\mu(r)$ at various distances far from the shower axis
- ✓ Muon production depth X^μ
- ✓ Shape of radial distribution of charged particles, electrons and muons (local slope η, lateral age parameter $s_\perp$ etc.)
- ✓ Shape of radial distribution of Cherenkov light
- ✓ Shape of radial distribution of EAS radio signal
- ✓ Distribution of the arrival time of charged particles in ground-based detectors (integral parameters of arrival time profiles)

Multicomponent methods using hybrid measurements, as well as deep learning based reconstruction procedures, are increasingly implemented

Cross-calibration between different mass-sensitive observables and different energy regions/different experiments is needed

Basic methods and techniques for primary mass estimations

Analysis of mean values, fluctuations, correlations or even particular features of distributions of different air shower observables characterized both longitudinal and spatial shower development

- ✓ Depth of maximum of the cascade curve $X_{\max}$
- ✓ Total number of electrons N_e and muons N_μ at the observation level, their correlation, muon size in inclined showers
- ✓ Local densities of electrons $\rho_e(r)$ and muons $\rho_\mu(r)$ at various distances far from the shower axis
- ✓ Muon production depth X^μ
- ✓ Shape of radial distribution of charged particles, electrons and muons (local slope η, lateral age parameter $s_\perp$ etc.)
- ✓ Shape of radial distribution of Cherenkov light
- ✓ Shape of radial distribution of EAS radio signal
- ✓ Distribution of the arrival time of charged particles in ground-based detectors (integral parameters of arrival time profiles)

Multicomponent methods using hybrid measurements, as well as deep learning based reconstruction procedures, are increasingly implemented

Cross-calibration between different mass-sensitive observables and different energy regions/different experiments is needed

Basic methods and techniques for primary mass estimations

Analysis of mean values, fluctuations, correlations or even particular features of distributions of different air shower observables characterized both longitudinal and spatial shower development

- ✓ Depth of maximum of the cascade curve $X_{\max}$
- ✓ Total number of electrons N_e and muons N_μ at the observation level, their correlation, muon size in inclined showers
- ✓ Local densities of electrons $\rho_e(r)$ and muons $\rho_\mu(r)$ at various distances far from the shower axis
- ✓ Muon production depth X^μ
- ✓ Shape of radial distribution of charged particles, electrons and muons (local slope η, lateral age parameter $s_\perp$ etc.)
- ✓ Shape of radial distribution of Cherenkov light
- ✓ Shape of radial distribution of EAS radio signal
- ✓ Distribution of the arrival time of charged particles in ground-based detectors (integral parameters of arrival time profiles)

Multicomponent methods using hybrid measurements, as well as deep learning based reconstruction procedures, are increasingly implemented

Cross-calibration between different mass-sensitive observables and different energy regions/different experiments is needed

Basic methods and techniques for primary mass estimations

Analysis of mean values, fluctuations, correlations or even particular features of distributions of different air shower observables characterized both longitudinal and spatial shower development

- ✓ Depth of maximum of the cascade curve $X_{\max}$
- ✓ Total number of electrons N_e and muons N_μ at the observation level, their correlation, muon size in inclined showers
- ✓ Local densities of electrons $\rho_e(r)$ and muons $\rho_\mu(r)$ at various distances far from the shower axis
- ✓ Muon production depth X^μ
- ✓ Shape of radial distribution of charged particles, electrons and muons (local slope η, lateral age parameter $s_\perp$ etc.)
- ✓ Shape of radial distribution of Cherenkov light
- ✓ Shape of radial distribution of EAS radio signal
- ✓ Distribution of the arrival time of charged particles in ground-based detectors (integral parameters of arrival time profiles)

Multicomponent methods using hybrid measurements, as well as deep learning based reconstruction procedures, are increasingly implemented

Cross-calibration between different mass-sensitive observables and different energy regions/different experiments is needed

Basic methods and techniques for primary mass estimations

Analysis of mean values, fluctuations, correlations or even particular features of distributions of different air shower observables characterized both longitudinal and spatial shower development

- ✓ Depth of maximum of the cascade curve $X_{\max}$
- ✓ Total number of electrons N_e and muons N_μ at the observation level, their correlation, muon size in inclined showers
- ✓ Local densities of electrons $\rho_e(r)$ and muons $\rho_\mu(r)$ at various distances far from the shower axis
- ✓ Muon production depth X^μ
- ✓ Shape of radial distribution of charged particles, electrons and muons (local slope η, lateral age parameter $s_\perp$ etc.)
- ✓ Shape of radial distribution of Cherenkov light
- ✓ Shape of radial distribution of EAS radio signal
- ✓ Distribution of the arrival time of charged particles in ground-based detectors (integral parameters of arrival time profiles)

Multicomponent methods using hybrid measurements, as well as deep learning based reconstruction procedures, are increasingly implemented

Cross-calibration between different mass-sensitive observables and different energy regions/different experiments is needed

Basic methods and techniques for primary mass estimations

Analysis of mean values, fluctuations, correlations or even particular features of distributions of different air shower observables characterized both longitudinal and spatial shower development

- ✓ Depth of maximum of the cascade curve $X_{\max}$
- ✓ Total number of electrons N_e and muons N_μ at the observation level, their correlation, muon size in inclined showers
- ✓ Local densities of electrons $\rho_e(r)$ and muons $\rho_\mu(r)$ at various distances far from the shower axis
- ✓ Muon production depth X^μ
- ✓ Shape of radial distribution of charged particles, electrons and muons (local slope η, lateral age parameter $s_\perp$ etc.)
- ✓ Shape of radial distribution of Cherenkov light
- ✓ Shape of radial distribution of EAS radio signal
- ✓ Distribution of the arrival time of charged particles in ground-based detectors (integral parameters of arrival time profiles)

Multicomponent methods using hybrid measurements, as well as deep learning based reconstruction procedures, are increasingly implemented

Cross-calibration between different mass-sensitive observables and different energy regions/different experiments is needed

Basic methods and techniques for primary mass estimations

Analysis of mean values, fluctuations, correlations or even particular features of distributions of different air shower observables characterized both longitudinal and spatial shower development

- ✓ Depth of maximum of the cascade curve $X_{\max}$
- ✓ Total number of electrons N_e and muons N_μ at the observation level, their correlation, muon size in inclined showers
- ✓ Local densities of electrons $\rho_e(r)$ and muons $\rho_\mu(r)$ at various distances far from the shower axis
- ✓ Muon production depth X^μ
- ✓ Shape of radial distribution of charged particles, electrons and muons (local slope η, lateral age parameter $s_\perp$ etc.)
- ✓ Shape of radial distribution of Cherenkov light
- ✓ Shape of radial distribution of EAS radio signal
- ✓ Distribution of the arrival time of charged particles in ground-based detectors (integral parameters of arrival time profiles)

Multicomponent methods using hybrid measurements, as well as deep learning based reconstruction procedures, are increasingly implemented

Cross-calibration between different mass-sensitive observables and different energy regions/different experiments is needed

Basic methods and techniques for primary mass estimations

Analysis of mean values, fluctuations, correlations or even particular features of distributions of different air shower observables characterized both longitudinal and spatial shower development

- ✓ Depth of maximum of the cascade curve $X_{\max}$
- ✓ Total number of electrons N_e and muons N_μ at the observation level, their correlation, muon size in inclined showers
- ✓ Local densities of electrons $\rho_e(r)$ and muons $\rho_\mu(r)$ at various distances far from the shower axis
- ✓ Muon production depth X^μ
- ✓ Shape of radial distribution of charged particles, electrons and muons (local slope η, lateral age parameter $s_\perp$ etc.)
- ✓ Shape of radial distribution of Cherenkov light
- ✓ Shape of radial distribution of EAS radio signal
- ✓ Distribution of the arrival time of charged particles in ground-based detectors (integral parameters of arrival time profiles)

Multicomponent methods using hybrid measurements, as well as deep learning based reconstruction procedures, are increasingly implemented

Cross-calibration between different mass-sensitive observables and different energy regions/different experiments is needed

Bibliography

1. Kampert K.-H., Unger M. Measurements of the cosmic ray composition with air shower experiments//Astropart. Phys. 2012. 35. 10.
2. Haungs A. Cosmic Rays from the Knee to the Ankle//Physics Procedia. 2015. 61.
3. Abbasi R.U., Abe M., Abu-Zayyad T. et al. Study of Ultra-High Energy Cosmic Ray composition using Telescope Array's Middle Drum detector and surface array in hybrid mode // Astropart. Phys. 2015. 64.
4. Yushkov A., Risse M., Werner M., Krieg J. Determination of the proton-to-helium ratio in cosmic rays at ultra-high energies from the tail of the Xmax distribution//Astropart. Phys. 2016. 85.
5. Aab A., Abreu P., Aglietta M. et al. Evidence for a mixed mass composition at the 'ankle' in the cosmic-ray spectrum//Physics Letters B. 2016. 762.
6. Buitink S., Corstanje A., Falcke H. et al. A large light-mass component of cosmic rays at $10^{17} - 10^{17.5}$ electronvolts from radio observations//Nature. 2016. 531.

Bibliography (II)

7. A. Yushkov. Recent results from the Pierre Auger Observatory on the mass composition and hadronic interactions of ultra-high energy cosmic rays//EPJ Web of Conferences. 2017. 145. 05002.
8. J.R. Hörandel, A. Bonardi, S. Buitink et al. The mass composition of cosmic rays measured with LOFAR//EPJ Web of Conferences. 2017. 136. 02001.
9. A. Aab et al. Combined fit of spectrum and composition data as measured by the Pierre Auger Observatory//JCAP04(2017)038
10. A. Chiavassa. Measurement of the cosmic ray spectrum and chemical composition in the $10^{15} - 10^{18}$ eV energy range//EPJ Web of Conferences. 2018. 172. 07001.
11. W. Hanlon, J. Bellido, J. Belz et al. Report of the Working Group on the Mass Composition of Ultrahigh Energy Cosmic Rays//JPS Conf. Proc. 2018. 19. 011013.
12. M. Erdmann, J. Glombitza, and D. Walz. A deep learning-based reconstruction of cosmic rayinduced air showers//Astropart. Phys. 97 (2018), pp. 46–53.

Bibliography (III)

13. I.S. Karpikov, G.I. Rubtsov, Ya.V. Zhezher. Lower limit on the ultrahigh-energy proton-tohelium ratio from the measurements of the tail of the Xmax distribution//Phys. Rev. D. 2018. 98. 10. 103002.
14. A. Yushkov, J, Bellido, J, Belz. Depth of maximum of air-shower profiles: testing the compatibility of measurements performed at the Pierre Auger Observatory and the Telescope Array experiment//EPJ Web of Conferences 210, 01009 (2019)
15. R.U. Abbasi et al. The Cosmic-Ray Composition between 2 PeV and 2 EeV Observed with the TALE Detector in Monocular Mode//ApJ. 2021. 909. 178
16. A. Aab et al. Deep-Learning based Reconstruction of the Shower Maximum X_{max} using the Water-Cherenkov Detectors of the Pierre Auger Observatory. arXiv:2101.02946v1 [astro-ph.IM]
17. A. Corstanje, S. Buitink, H. Falcke et al. Depth of shower maximum and mass composition of cosmic rays from 50 PeV to 2 EeV measured with the LOFAR radio telescope//Phys. Rev. D 103, 102006. 2021
18. P. Lipari. Spectra and composition of ultrahigh-energy cosmic rays and the measurement of the proton-air cross section//Phys. Rev. D 103, 103009. 2021

Despite large efforts that have been made recently the composition results remain ambiguous in almost the entire energy range available for EAS studies

Main constraints

- Lack of statistics at highest energies (low duty cycle of FD)
- Hadronic interaction model uncertainties
- The “Muon Puzzle” (models show a significant muon deficit with respect to measurements)
- Self-consistency problem (e.g. $\langle \ln A \rangle$ from FD and SD disagree; *Yushkov A., 2019*)
- Complex of mixed instrumental and methodical systematic biases of different nature and specific for concrete experiment (detector properties, meteorological effects etc.). As a consequence, uncertainties during cross-calibration between different observables and different experiments.

Uncertain mass composition is the main obstacle to physically interpreting the CR data in terms of sources and propagation models

Possible way-outs

- Improved statistics and (multi-)hybrid measurements with upgraded configurations of current arrays (AugerPrime, TALE, TAx4, TAIGA, Yakutsk etc.), including the potential for effective discriminating between electron and muon contributions in the local charged particle densities.
- Development of (new?) methods to infer the composition with precision comparable to that of fluorescence detectors and at a duty cycle of almost 100%
- Decrease the theoretical uncertainties on the mass composition due to our limited understanding of hadronic interactions and mixed systematics by using the universal, theoretically motivated, properties of shower development as a basis primary particle discrimination, instead of the 'black box' techniques
- New experiments, such as POEMMA, CRAFFT, FAST, GRAND, GCOS, with apertures of more than one order of magnitude larger than that of Auger (currently in the design stage)

Scaling formalism for lateral distributions

Nishimura-Kamata-Greizen Function (Nishimura J. and Kamata K., 1958; Greisen K., 1960)

$$\rho(r;E,s) = N(E,s)\frac{C}{r_0^2}\left(\frac{r}{r_0}\right)^{s-2}\left(1+\frac{r}{r_0}\right)^{s-4.5}. \quad (1)$$

$s = 3X/(X+2X_{\max})$, r_0 – constant shower scale radius (originally the Moliere unit r_M).

Not sufficient at large radial distances (*Lagutin A.A. et al. 1979*).

Modifications of the NKG form

- changing the values of exponents
- different constant or variable scale factors
- lateral ($s_\perp$) or local ($s(r)$) age parameters
- introducing a third power-law term

Yoshida S. et al., 1994; Capdevielle J.N. et al., 2002; Apel W. et al., 2006; Dey R.K. et al., 2012, 2016; Tapia A. et al., 2013; Bartoli B. et al., 2017

Scaling formalism for lateral distributions (II)

Scaling Lateral Distribution Function

$$\rho(r; E, X) = \frac{N(E, X)}{R_0^2(E, X)} F\left(\frac{r}{R_0(E, X)}\right). \quad (2)$$

$F(r/R_0)$ – scaling function; $R_0(E, X)$ – scale factor.

Scaling Function $(x = r/R_0)$

$$F(x) = Cx^{-\alpha}(1 + x)^{-(\beta-\alpha)}\left(1 + \left(\frac{x}{10}\right)^{\gamma}\right)^{-\delta}. \quad (3)$$

Set of parameters (same for electron LDF in photon- and nicleus- induces showers):
$C = 0.28, \alpha = 1.2, \beta = 4.53, \gamma = 2.0, \delta = 0.6$.

$R_0 = R_{\text{ms}}$ – mean square radius of electron component:

$$R^2_{\text{ms}}(E, X) = \frac{2\pi}{N_e(E, t)} \int_0^\infty r^2 \rho_e(r; E,) r dr$$

Scaling formalism for lateral distributions (III)

Electron LDF

$$\rho(r;E,X) = N(E,X)\frac{0.28}{R_0^2(E,X)}\left(\frac{r}{R_0}\right)^{\boxed{-1.2}}\left(1+\frac{r}{R_0}\right)^{\boxed{-3.33}}\left(1+\left(\frac{r}{10R_0}\right)^2\right)^{\boxed{-0.6}} \quad (4)$$

Muon LDF implemented at KASCADE-Grande, $R_0 = 320$ m (*Apel W.D. et al. 2017*)

$$\rho(r;E,X) = N(E,X)\frac{0.28}{R_0^2(E,X)}\left(\frac{r}{R_0}\right)^{\boxed{-0.69}}\left(1+\frac{r}{R_0}\right)^{\boxed{-2.39}}\left(1+\left(\frac{r}{10R_0}\right)^2\right)^{\boxed{-1.0}} \quad (5)$$

Confirmation by KASCADE

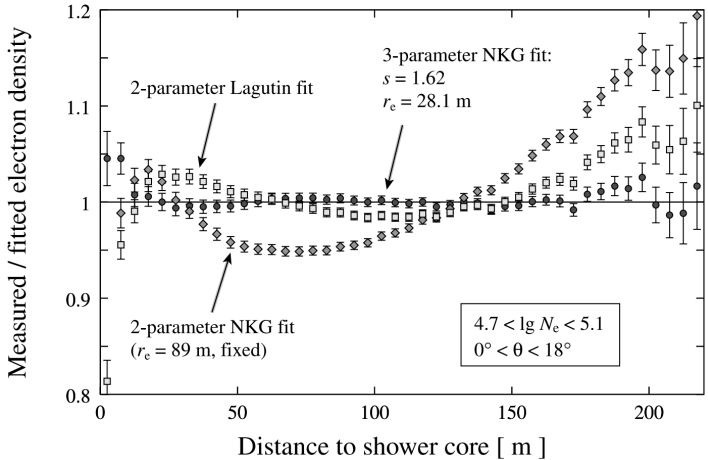

Residuals in the ratio of measured over fitted average LDF (*Antoni T. et al., 2001*)

LDF of Electrons (> 1 MeV). Scaling Function Fit

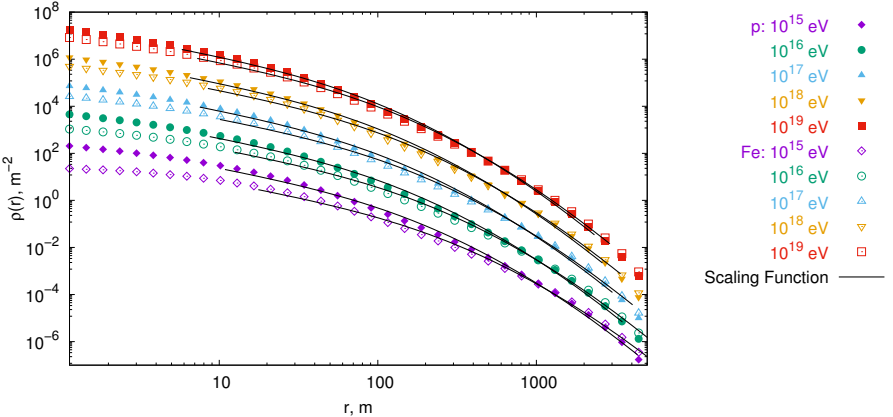

CORSIKA v. 7.4100; EPOS-LHC v.3400; FLUKA 2011.2c.2; thinning level $E_i/E_0 = 10^{-8}$; weight limit $w_{\max} = 10^2$

LDF of Electrons (> 1 MeV). Scaling Function Fit (II)

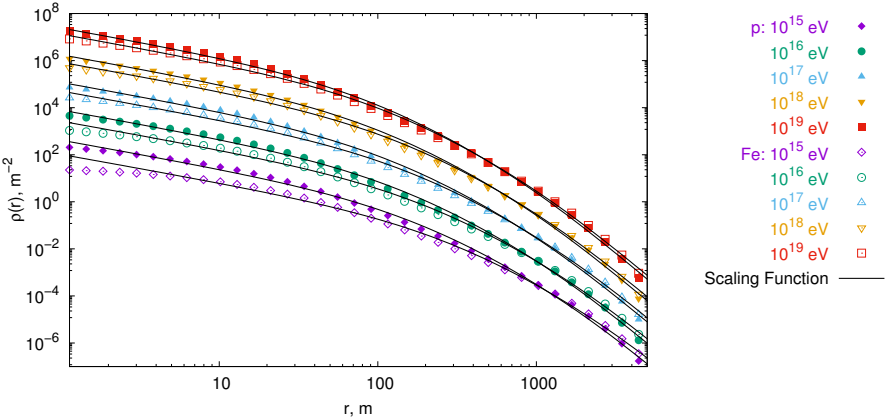

CORSIKA v. 7.4100; EPOS-LHC v.3400; FLUKA 2011.2c.2; thinning level $E_i/E_0 = 10^{-8}$; weight limit $w_{\max} = 10^2$

LDF of Electrons (> 1 MeV). Scaling Function Fit (III)

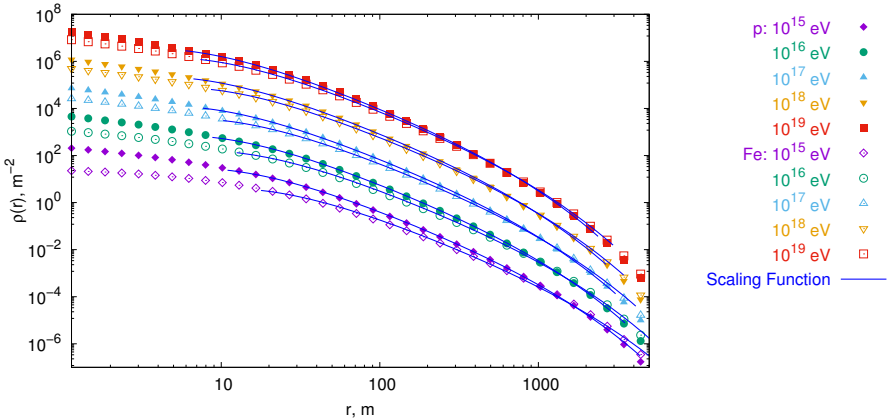

CORSIKA v. 7.4100; EPOS-LHC v.3400; FLUKA 2011.2c.2; thinning level $E_i/E_0 = 10^{-8}$; weight limit $w_{\max} = 10^2$

LDF of Muons (> 10 MeV). Scaling Function Fit

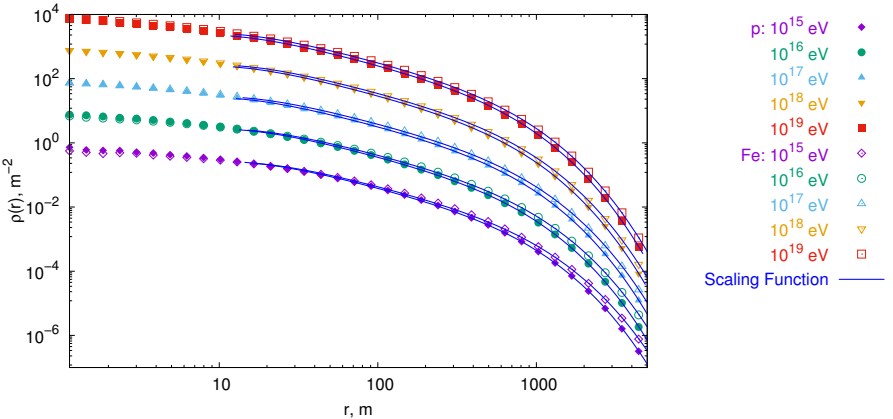

CORSIKA v. 7.4100; EPOS-LHC v.3400; FLUKA 2011.2c.2; thinning level $E_i/E_0 = 10^{-8}$; weight limit $w_{\max} = 10^2$

Scaling Part of the LDF

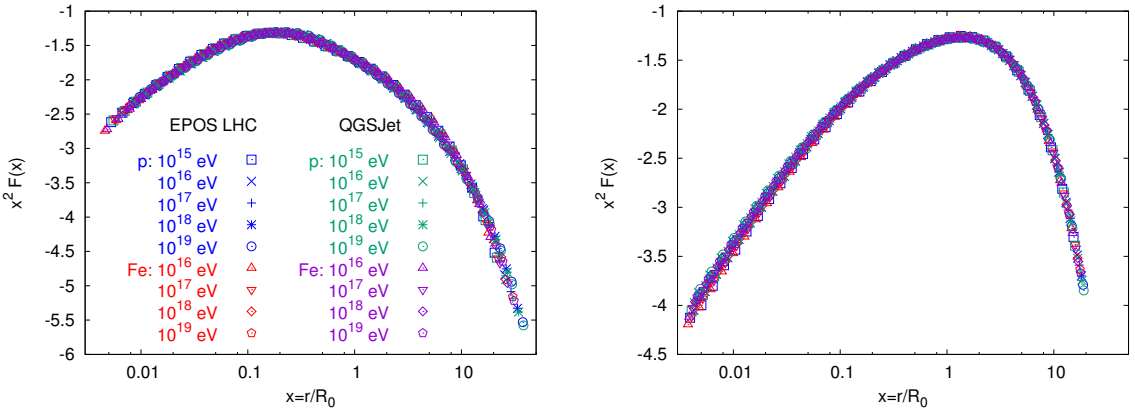

Invariant part of average lateral distribution of electrons (left) and muons (right) at sea level for vertical simulated EAS.

Scaling Part of the LDF

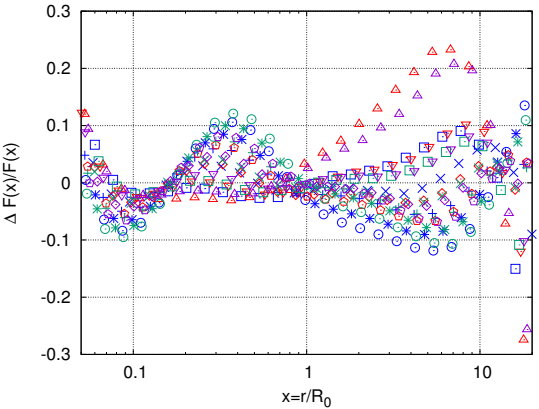

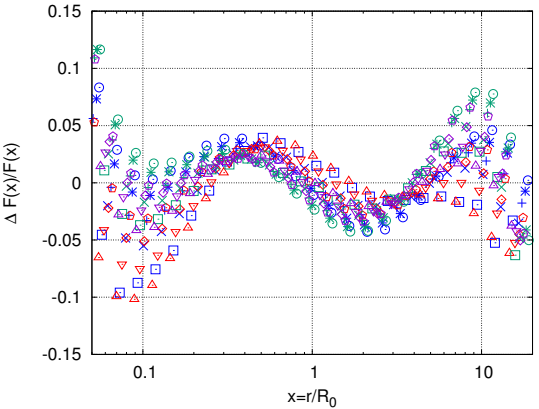

Relative uncertainties of the scaling description of average lateral distribution of electrons (left) and muons (right) at sea level for vertical simulated EAS.

Limitations (electron component)

Simulated LDF are reproduced with the accuracy $\leq$15% in the range of $x = (0.05 \div 20)$

Photon-generated electromagnetic showers: $E = (10^9 \div 10^{22})$ eV, $s = (0.6 \div 1.6)$.
EAS initiated by nuclei: $E = (10^{15} \div 10^{19})$ eV, $(600 \div 1030)$ g/cm^2.

Insensitivity to the hadronic interaction model!

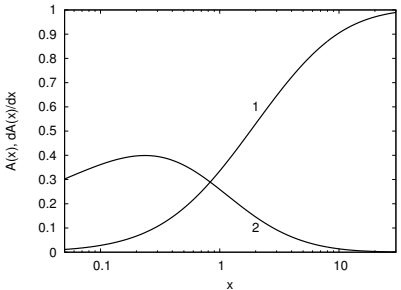

$$A(x) = \frac{R^{\rm tr}_{\rm ms}(0, xR_{\rm ms})}{R_{\rm ms}} = \left[2\pi \int_0^x x'^3\, F(x')dx'\right]^{1/2}, \frac{dA(x)}{dx}$$

Values of $r = xR_{\rm ms}$ (m) for proton-induced EAS at sea level (CORSIKA/EPOS-LHC).

x	10^{15} eV	10^{17} eV	10^{19} eV
0.05	11.0	7.7	5.9
0.24	52.6	36.9	28.5
20.0	4383	3071	2379

Implementations at moderate energies

- KASCADE (*T. Antoni et al., 2001*)
- MSU (*N. N. Kalmykov et al., 2007; Yu. A. Fomin et al., 2008*)
- KASCADE-Grande (*F. Di Pierro et al., 2009; V. de Souza et al., 2009; D. Fuhrmann et al., 2009*)

KASCADE

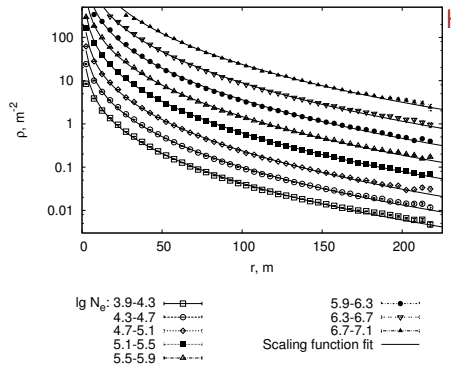

MSU Array

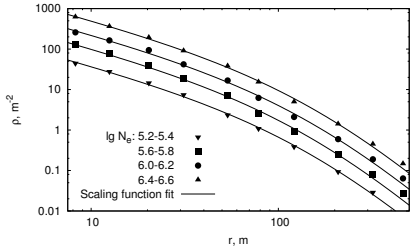

KASCADE-Grande

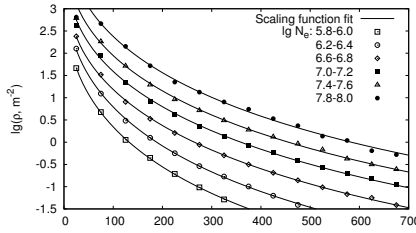

Raikin R.I. et al.//Nucl. Phys. B (Proc. Suppl.) 196 (2009) 383–386; Raikin R.I. et al.//Proc. 32 ICRC, Beijing, 2011, Vol. 1. 299-302.

Implementations at moderate energies

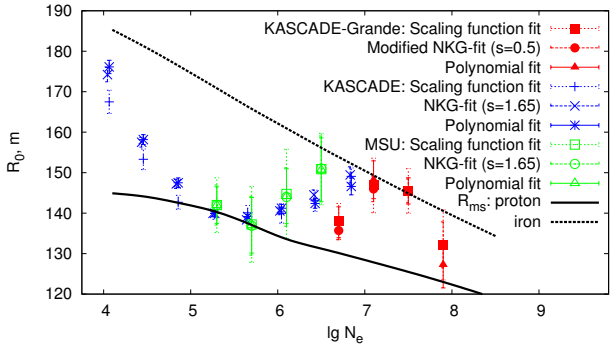

Cross-calibration between KASCADE, MSU Array and KASCADE-Grande. Consistency irrespective of the concrete form of LDF scaling part. “Iron knee” hint.

Raikin R.I. et al.//Nucl. Phys. B (Proc. Suppl.) 196 (2009) 383–386; Raikin R.I. et al.//Proc. 32 ICRC, Beijing, 2011, Vol. 1. 299-302.

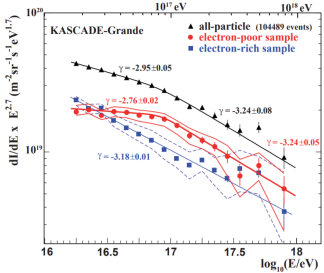

Apel W.D. et al. 2011 (Kneelike structure in the spectrum of the heavy component of cosmic rays observed with KASCADE-Grande)

Perspectives for extremely-high energies

Effects that should be taken into account:

π^0 nuclear interactions

Landau-Pomeranchuk-Migdal (LPM) effect

Interactions of primary gamma-quanta (if any) with geomagnetic field (GMF-effect)

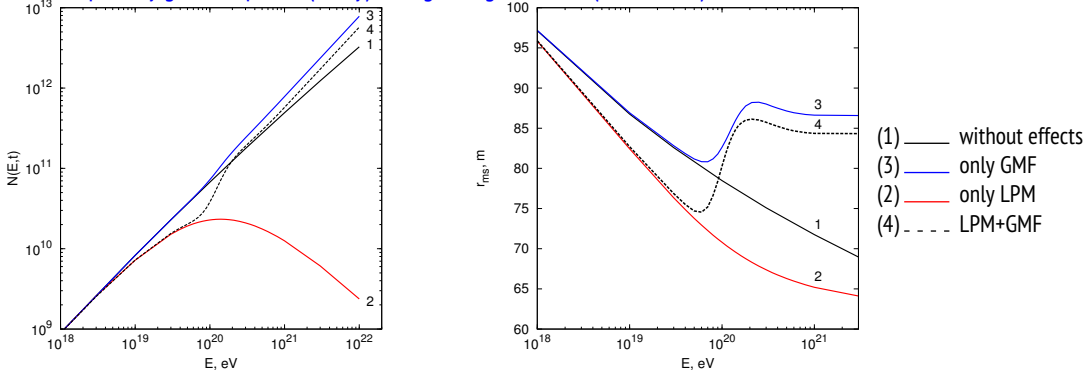

Energy dependences of the N_e (left) and r_{ms} (right) of electron component in vertical electromagnetic air showers induced by photons with $E_\gamma = (10^{18} \div 10^{22})$ eV at 890 g/cm^2 with and without taking into account the UHE-effects. The GMF intensity profile corresponds to the PAO location *(Serebryakova T.L. et al., 2019)*

Universality

Scaling factors R_0 of LDF of electrons (bottom) and muons (top) at sea level vs $X_{\max}$. Approximation curves correspond to EPOS LHC v.3400 (solid) and QGSJet-II-04 (dashed).

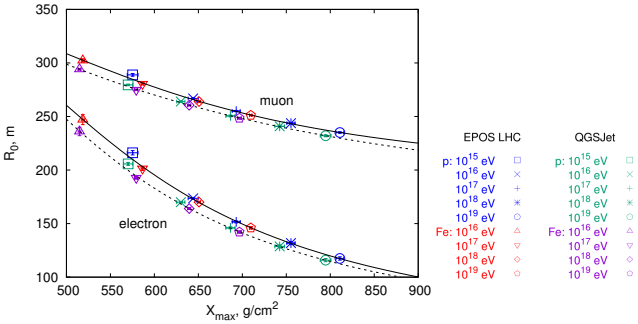

Parameters of average vertical EAS generated by p and Fe in the energy range of $(10^{15} \div 10^{19})$ eV for EPOS LHC and QGSJet.

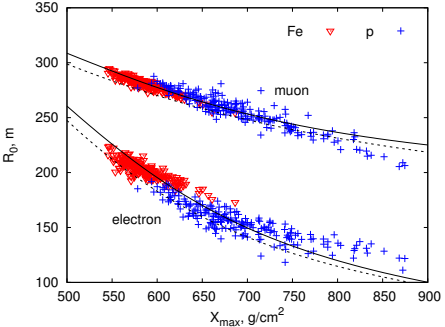

Scatter plot with parameters of individual EAS generated by p and Fe (10^{17} eV; EPOS LHC)

Distributions of $X_{\max}$ and R_0 (electrons, sea level)

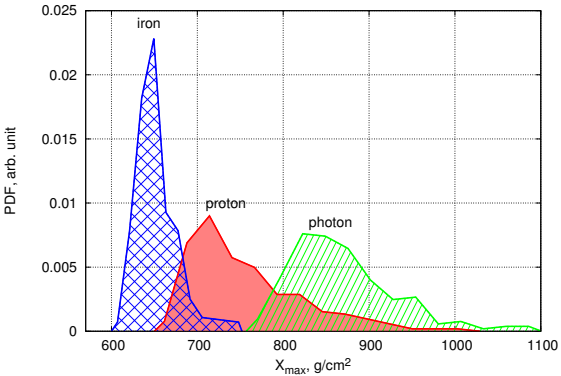

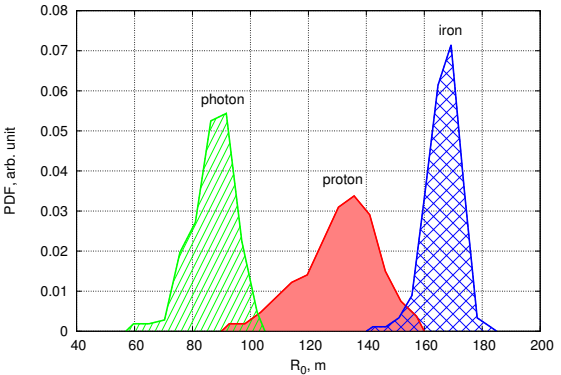

200 simulated vertical showers from photons, protons and iron at 10^{18} eV (EPOS-LHC)

$R_0^{r_1-r_2}$ estimations

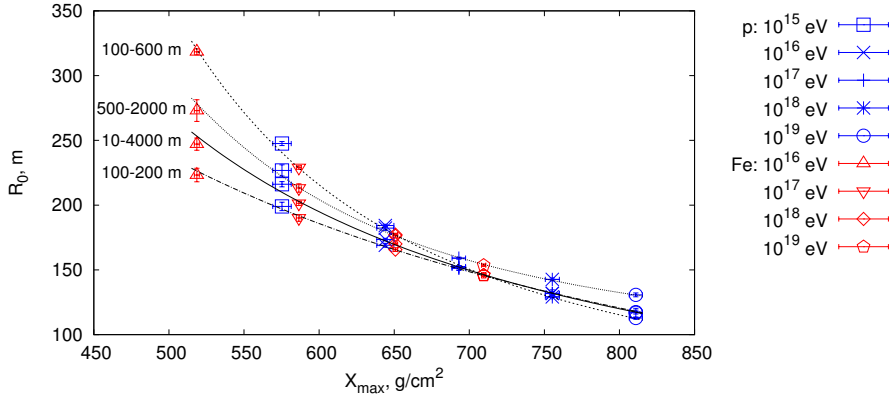

$(10^{15} \div 10^{19})$ eV, EPOS LHC

Time profiles of EAS particles in surface detectors

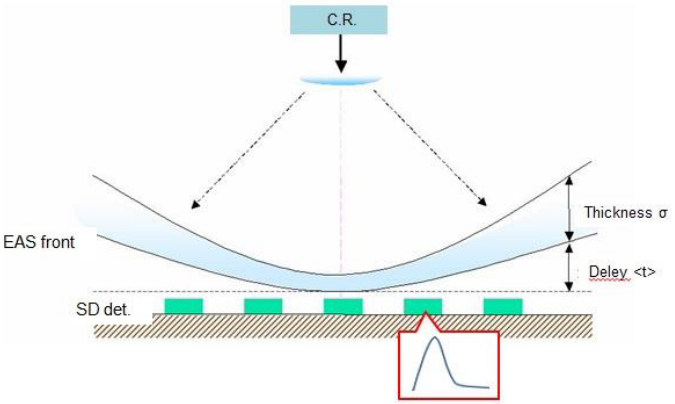

Promising as rather irrespective from the shape of lateral distribution channel of information about primary particle

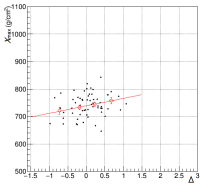

TA *(Inoue N. et al., 2015)*

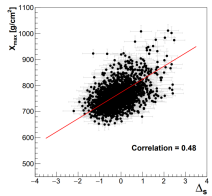

PAO *(Peixoto C.J.T. et al., 2019)*

Conclusions

1. Uncertainty of the CR mass composition is the main obstacle to physically interpreting features of the energy spectrum, detecting the transitional between galactic and extragalactic CR, improve our knowledges about hadronic interactions at energies way beyond human-made accelerators, and eventually discriminating between models of CR acceleration and propagation
2. Hopes for the nearest future are primarily associated with the improved measurements by the upgraded facilities and, at the same time, with the development of methods that are robust with respect to the hadronic interaction model (it is very important to use the potential of ground-based detectors with 100% duty cycle)
3. LDF of electrons and muons in air showers are scale-invariant in wide primary energy and radial distance ranges. Scaling formalism is valid up to the extremely high energies (if the absence of a new physics is assumed)
4. The scale-invariance of LDF and air shower universality manifesting through the functional dependence between radial scale factors and longitudinal shower age as qualitative features are both insensitive to hadronic interaction model
5. The use of the scale factors R_0 of the LDF of electrons and muons as primary mass indicators is possible both on the averaged and event-by-event basis at different experiments, which opens up possibilities for improving the accuracy of reconstructing the mass composition, as well as for reanalysis and verification of the consistency of data from various experiments, their calibration and validation
6. In combination with the time profile (rise-time) technique the proposed approach could be a powerful tool towards model-independent mass composition evaluation at AugerPrime, TALE, Tax4, TAIGA, Yakutsk Complex Air Shower Array

Conclusions

1. Uncertainty of the CR mass composition is the main obstacle to physically interpreting features of the energy spectrum, detecting the transitional between galactic and extragalactic CR, improve our knowledges about hadronic interactions at energies way beyond human-made accelerators, and eventually discriminating between models of CR acceleration and propagation
2. Hopes for the nearest future are primarily associated with the improved measurements by the upgraded facilities and, at the same time, with the development of methods that are robust with respect to the hadronic interaction model (it is very important to use the potential of ground-based detectors with 100% duty cycle)
3. LDF of electrons and muons in air showers are scale-invariant in wide primary energy and radial distance ranges. Scaling formalism is valid up to the extremely high energies (if the absence of a new physics is assumed)
4. The scale-invariance of LDF and air shower universality manifesting through the functional dependence between radial scale factors and longitudinal shower age as qualitative features are both insensitive to hadronic interaction model
5. The use of the scale factors R_0 of the LDF of electrons and muons as primary mass indicators is possible both on the averaged and event-by-event basis at different experiments, which opens up possibilities for improving the accuracy of reconstructing the mass composition, as well as for reanalysis and verification of the consistency of data from various experiments, their calibration and validation
6. In combination with the time profile (rise-time) technique the proposed approach could be a powerful tool towards model-independent mass composition evaluation at AugerPrime, TALE, Tax4, TAIGA, Yakutsk Complex Air Shower Array

Conclusions

1. Uncertainty of the CR mass composition is the main obstacle to physically interpreting features of the energy spectrum, detecting the transitional between galactic and extragalactic CR, improve our knowledges about hadronic interactions at energies way beyond human-made accelerators, and eventually discriminating between models of CR acceleration and propagation
2. Hopes for the nearest future are primarily associated with the improved measurements by the upgraded facilities and, at the same time, with the development of methods that are robust with respect to the hadronic interaction model (it is very important to use the potential of ground-based detectors with 100% duty cycle)
3. LDF of electrons and muons in air showers are scale-invariant in wide primary energy and radial distance ranges. Scaling formalism is valid up to the extremely high energies (if the absence of a new physics is assumed)
4. The scale-invariance of LDF and air shower universality manifesting through the functional dependence between radial scale factors and longitudinal shower age as qualitative features are both insensitive to hadronic interaction model
5. The use of the scale factors R_0 of the LDF of electrons and muons as primary mass indicators is possible both on the averaged and event-by-event basis at different experiments, which opens up possibilities for improving the accuracy of reconstructing the mass composition, as well as for reanalysis and verification of the consistency of data from various experiments, their calibration and validation
6. In combination with the time profile (rise-time) technique the proposed approach could be a powerful tool towards model-independent mass composition evaluation at AugerPrime, TALE, Tax4, TAIGA, Yakutsk Complex Air Shower Array

Conclusions

1. Uncertainty of the CR mass composition is the main obstacle to physically interpreting features of the energy spectrum, detecting the transitional between galactic and extragalactic CR, improve our knowledges about hadronic interactions at energies way beyond human-made accelerators, and eventually discriminating between models of CR acceleration and propagation
2. Hopes for the nearest future are primarily associated with the improved measurements by the upgraded facilities and, at the same time, with the development of methods that are robust with respect to the hadronic interaction model (it is very important to use the potential of ground-based detectors with 100% duty cycle)
3. LDF of electrons and muons in air showers are scale-invariant in wide primary energy and radial distance ranges. Scaling formalism is valid up to the extremely high energies (if the absence of a new physics is assumed)
4. The scale-invariance of LDF and air shower universality manifesting through the functional dependence between radial scale factors and longitudinal shower age as qualitative features are both insensitive to hadronic interaction model
5. The use of the scale factors R_0 of the LDF of electrons and muons as primary mass indicators is possible both on the averaged and event-by-event basis at different experiments, which opens up possibilities for improving the accuracy of reconstructing the mass composition, as well as for reanalysis and verification of the consistency of data from various experiments, their calibration and validation
6. In combination with the time profile (rise-time) technique the proposed approach could be a powerful tool towards model-independent mass composition evaluation at AugerPrime, TALE, Tax4, TAIGA, Yakutsk Complex Air Shower Array

Conclusions

1. Uncertainty of the CR mass composition is the main obstacle to physically interpreting features of the energy spectrum, detecting the transitional between galactic and extragalactic CR, improve our knowledges about hadronic interactions at energies way beyond human-made accelerators, and eventually discriminating between models of CR acceleration and propagation
2. Hopes for the nearest future are primarily associated with the improved measurements by the upgraded facilities and, at the same time, with the development of methods that are robust with respect to the hadronic interaction model (it is very important to use the potential of ground-based detectors with 100% duty cycle)
3. LDF of electrons and muons in air showers are scale-invariant in wide primary energy and radial distance ranges. Scaling formalism is valid up to the extremely high energies (if the absence of a new physics is assumed)
4. The scale-invariance of LDF and air shower universality manifesting through the functional dependence between radial scale factors and longitudinal shower age as qualitative features are both insensitive to hadronic interaction model
5. The use of the scale factors R_0 of the LDF of electrons and muons as primary mass indicators is possible both on the averaged and event-by-event basis at different experiments, which opens up possibilities for improving the accuracy of reconstructing the mass composition, as well as for reanalysis and verification of the consistency of data from various experiments, their calibration and validation
6. In combination with the time profile (rise-time) technique the proposed approach could be a powerful tool towards model-independent mass composition evaluation at AugerPrime, TALE, Tax4, TAIGA, Yakutsk Complex Air Shower Array

Conclusions

1. Uncertainty of the CR mass composition is the main obstacle to physically interpreting features of the energy spectrum, detecting the transitional between galactic and extragalactic CR, improve our knowledges about hadronic interactions at energies way beyond human-made accelerators, and eventually discriminating between models of CR acceleration and propagation
2. Hopes for the nearest future are primarily associated with the improved measurements by the upgraded facilities and, at the same time, with the development of methods that are robust with respect to the hadronic interaction model (it is very important to use the potential of ground-based detectors with 100% duty cycle)
3. LDF of electrons and muons in air showers are scale-invariant in wide primary energy and radial distance ranges. Scaling formalism is valid up to the extremely high energies (if the absence of a new physics is assumed)
4. The scale-invariance of LDF and air shower universality manifesting through the functional dependence between radial scale factors and longitudinal shower age as qualitative features are both insensitive to hadronic interaction model
5. The use of the scale factors R_0 of the LDF of electrons and muons as primary mass indicators is possible both on the averaged and event-by-event basis at different experiments, which opens up possibilities for improving the accuracy of reconstructing the mass composition, as well as for reanalysis and verification of the consistency of data from various experiments, their calibration and validation
6. In combination with the time profile (rise-time) technique the proposed approach could be a powerful tool towards model-independent mass composition evaluation at AugerPrime, TALE, Tax4, TAIGA, Yakutsk Complex Air Shower Array

Acknowledgement

Authors are greatly indebted to *Dr. Alexey Yushkov* from Auger Collaboration
for valuable discussions and materials provided.

Results presented here were partially supported
by Russian Foundation for Basic Research (RFBR) Grant (16-02-01103).

Thanks for your attention!